First observation of the decay B-s(0) -> (KSK)-K-0*(892)(0) at LHCb

LHCb Collaboration; Onderwater, C. J. G.; Pellegrino, A. ; Tolk, S.

Published in:
Journal of High Energy Physics

DOI:
10.1007/JHEP01(2016)012

Publication date:
2016

Published for SISSA by Springer

Received: *July 2, 2015*
Revised: *November 4, 2015*
Accepted: *December 15, 2015*
Published: *January 4, 2016*

First observation of the decay $B_s^0 \to K_S^0 K^*(892)^0$ at LHCb

The LHCb collaboration

E-mail: marianna.fontana@cern.ch

Abstract: A search for $B^0_{(s)} \to K^0_S K^*(892)^0$ decays is performed using pp collision data, corresponding to an integrated luminosity of 1.0 fb^{-1}, collected with the LHCb detector at a centre-of-mass energy of 7 TeV. The $B^0_s \to K^0_S K^*(892)^0$ decay is observed for the first time, with a significance of 7.1 standard deviations. The branching fraction is measured to be

$$\mathcal{B}(B^0_s \to \bar{K}^0 K^*(892)^0) + \mathcal{B}(B^0_s \to K^0 \bar{K}^*(892)^0) = (16.4 \pm 3.4 \pm 2.3) \times 10^{-6},$$

where the first uncertainty is statistical and the second is systematic. No evidence is found for the decay $B^0 \to K^0_S K^*(892)^0$ and an upper limit is set on the branching fraction, $\mathcal{B}(B^0 \to \bar{K}^0 K^*(892)^0) + \mathcal{B}(B^0 \to K^0 \bar{K}^*(892)^0) < 0.96 \times 10^{-6}$, at 90 % confidence level. All results are consistent with Standard Model predictions.

Keywords: Hadron-Hadron scattering, B physics

ArXiv ePrint: 1506.08634

doi:10.1007/JHEP01(2016)012

JHEP01(2016)012

Contents

JHEP01(2016)012

1 Introduction

Violation of the combined charge-conjugation and parity symmetry (CP) is one of the fundamental ingredients to explain a dynamical generation of the observed matter-antimatter asymmetry in the universe [1]. In the Standard Model of particle physics (SM), CP violation in the quark sector is generated by a single complex phase in the Cabibbo-Kobayashi-Maskawa matrix [2, 3]. However, the observed baryon asymmetry is too large to be explained by the SM mechanism alone [4]. Non-leptonic B meson decays dominated by amplitudes involving a quark and a W boson in a loop (penguin) are sensitive to the presence of non-SM physics processes. These processes could provide additional sources of CP violation that might explain the observed baryon asymmetry. The $B^0_{(s)} \to K^0_S h^\pm h'^\mp$ $(h, h' = \pi, K)$ decays are interesting for CP violation measurements.[1] Knowledge of the branching fractions of the various sub-modes, as reported in this paper, is an important input to the theory of CP-violation, particularly models of new-physics contributions to $b \to s$ transitions ref. [5] . The measurements also allow tests of QCD models (see, for example, the predictions in refs. [6–8]). If sufficient data are available, a common approach for three-body decays is to perform an amplitude analysis by studying the structure of the Dalitz plot [9]. If data are less abundant and the decay products originate from intermediate resonances, as in the present analysis, a quasi two-body approach can be used.

The LHCb collaboration has provided results for inclusive $B^0_{(s)} \to K^0_S h^\pm h'^\mp$ decays [10], and more recently the first measurements of B^0_s meson decays to $K^*(892)^-\pi^+$ and $K^*(892)^-K^+$ final states [11]. An initial search for the neutral decay $B^0 \to K^*(892)^0 K^0_S$ has been reported by the BaBar experiment [12]. In this paper a search for $B^0_{(s)} \to$

[1] Charge-conjugate modes are implicitly included throughout this paper.

$K^0_S K^*(892)^0$ decays is reported, where the $K^*(892)^0$ meson, hereafter denoted by K^{*0}, decays to the $K^+\pi^-$ final state. The resonant structure in the $K^+\pi^-$ invariant mass region around $1\,\text{GeV}/c^2$ is analysed to determine the number of decays that proceed through an intermediate K^{*0} resonance. The branching fraction is measured relative to the $B^0 \to K^0_S\pi^+\pi^-$ decay [13], using the relation

$$\frac{\mathcal{B}(B^0_{(s)} \to K^0_S K^{*0})}{\mathcal{B}(B^0 \to K^0_S\pi^+\pi^-)} = \frac{N_{B^0_{(s)}\to K^0_S K^{*0}}}{N_{B^0\to K^0_S\pi^+\pi^-}} \cdot \frac{\epsilon_{B^0\to K^0_S\pi^+\pi^-}}{\epsilon_{B^0_{(s)}\to K^0_S K^{*0}}} \cdot \frac{f_d}{f_{d(s)}} \cdot \frac{1}{\mathcal{B}(K^{*0} \to K^+\pi^-)}, \tag{1.1}$$

where N represents the number of observed decays, ϵ the total efficiency, and f_s/f_d the ratio of the fragmentation fractions of a b quark into a B^0_s or a B^0 meson [14–16] and $\mathcal{B}(K^{*0} \to K^+\pi^-)$ is the branching fraction of the K^{*0} meson into $K^+\pi^-$ final state. In the following, the $B^0_{(s)} \to K^0_S K^{*0}$ and $B^0 \to K^0_S\pi^+\pi^-$ decays are referred to as signal and normalisation channels, respectively.

2 Detector and simulation

The analysis is performed using pp collision data recorded with the LHCb detector, corresponding to an integrated luminosity of $1.0\,\text{fb}^{-1}$, at a centre-of-mass energy of 7TeV. The LHCb detector [17, 18] is a single-arm forward spectrometer covering the pseudorapidity range $2 < \eta < 5$, designed for the study of particles containing b or c quarks. The detector includes a high-precision tracking system consisting of a silicon-strip vertex detector surrounding the pp interaction region, a large-area silicon-strip detector located upstream of a dipole magnet with a bending power of about 4 Tm, and three stations of silicon-strip detectors and straw drift tubes placed downstream of the magnet. The tracking system provides a measurement of momentum, p, of charged particles with a relative uncertainty that varies from 0.5% at low momentum to 1.0% at $200\,\text{GeV}/c$. The minimum distance of a track to a primary vertex (PV), the impact parameter, is measured with a resolution of $(15 + 29/p_\text{T})\,\mu\text{m}$, where p_T is the component of the momentum transverse to the beam, in GeV/c. Different types of charged hadrons are distinguished using information from two ring-imaging Cherenkov detectors. Photons, electrons and hadrons are identified by a calorimeter system consisting of scintillating-pad and preshower detectors, an electromagnetic calorimeter and a hadronic calorimeter. Muons are identified by a system composed of alternating layers of iron and multiwire proportional chambers.

Simulated events are used to determine the efficiency of the selection requirements, to study possible sources of background and to determine the parametrisations used to model the data. In the simulation, pp collisions are generated using Pythia 6 [19] with a specific LHCb configuration [20]. Decays of hadronic particles are described by EvtGen [21], in which final-state radiation is generated using Photos [22]. The interaction of the generated particles with the detector, and its response, are implemented using the Geant4 toolkit [23, 24] as described in ref. [25].

3 Event selection

The online event selection system (trigger) [26] consists of a hardware stage, based on information from the calorimeter and muon systems, followed by a software stage, in which

JHEP01(2016)012

all charged particles with $p_{\rm T} > 500\,{\rm MeV}/c$ are reconstructed. The hardware hadron trigger requires a calorimeter cluster with transverse energy greater than 3.5 GeV. In the offline selection, candidates are divided into two non mutually exclusive categories based on the hardware trigger decision. One category consists of candidates whose decay products satisfy the hadron trigger requirements, while the other consists of candidates from events in which other particles meet the hardware trigger requirements. Only events that fall into either of these categories are used in the subsequent analysis. The software trigger requires a two-, three- or four-particle secondary vertex with a significant displacement from the primary pp interaction points. At least one charged particle must have $p_{\rm T} > 1.7\,{\rm GeV}/c$ and be inconsistent with originating from any PV. A multivariate algorithm [27] is used for the identification of secondary vertices consistent with the decay of a b hadron.

In the offline selection the $B^0_{(s)} \to K^0_{\rm S} K^{*0}$ decays are reconstructed through the $K^{*0} \to K^+\pi^-$ and $K^0_{\rm S} \to \pi^+\pi^-$ decay modes, where the $K^0_{\rm S}$ candidate is constrained to its known mass [13] and the B candidate is constrained to originate from a PV. Decays of $K^0_{\rm S}$ mesons are reconstructed in two mutually exclusive categories: *long* $K^0_{\rm S}$ candidates, which decay sufficiently early that their daughter pions are reconstructed in the vertex detector; and *downstream* $K^0_{\rm S}$ candidates, which have daughter particles that are only reconstructed in the rest of the tracking system. As these two categories have different backgrounds, and the long $K^0_{\rm S}$ mesons have better momentum and vertex resolutions, the selection criteria for long and downstream $K^0_{\rm S}$ candidates differ. The selection criteria follow those in ref. [10].

Fully reconstructed background decays that have the same final state as the signal include contributions from B decays to final states involving charm mesons, such as Dh, with a $K^0_{\rm S}h^+h^-$ final state, or Λ^0_b decays to $\Lambda^+_c h^-$, with $\Lambda^+_c \to K^0_{\rm S} p$, where the proton is misidentified as a π^+ or K^+. In addition, B decays with an intermediate charmonium state like $B^0 \to J/\psi K^0_{\rm S}$, with $J/\psi \to \pi^+\pi^-, K^+K^-, \mu^+\mu^-$, can be present in the mass region of the normalisation channel. To reduce the contamination from these backgrounds, a veto is applied on the invariant mass of each of the possible intermediate states reconstructed under the corresponding hypothesis. Candidates are excluded if the reconstructed mass of a two-body intermediate state is within $30\,{\rm MeV}/c^2$ ($48\,{\rm MeV}/c^2$) of the known mass of the relevant intermediate charm (charmonium) resonance [13] of one of the backgrounds considered. No particle identification information is used at this stage.

If a final-state hadron is misidentified, signal yields can potentially be affected by decays into any $K^0_{\rm S}h^\pm h'^\mp$ final state, especially when the $h^\pm h'^\mp$ proceeds through a resonance. Particle identification requirements on the two tracks originating from the B decay vertex are used to separate pions, kaons and protons, and to reduce this background to a negligible level. The largest source of background is due to random tracks that form candidate B or $K^0_{\rm S}$ decay vertices. A multivariate discriminant based on a boosted decision tree (BDT) algorithm [28, 29] is used to reduce this background. The greatest discrimination in the BDT is provided by kinematic properties of the B meson, its flight direction with respect to the PV, and variables defined analogously for its decay products. The optimisation of the BDT is described in ref. [10]; the selection requirement on the BDT response for this analysis is chosen to maximise $\epsilon/(a/2 + \sqrt{N_B})$ [30]. Here, ϵ is the signal efficiency, B represents the number of background events in the signal mass interval, which is estimated

JHEP01(2016)012

using data by extrapolating the number of background events from the upper mass sideband into the signal region, and $a = 5$ is the chosen target signal significance.

The efficiencies are determined from simulation, except for the particle identification efficiencies. The latter are determined from data using samples of kinematically identified charged particles from $D^{*+} \to D^0\pi^+$ with $D^0 \to K^-\pi^+$, and $\Lambda \to \pi^- p$ decays, reweighted to match the kinematic properties of the signal. The BDT selection efficiency for signal is approximately 85% (90%) for downstream (long) signal decays; approximately 88% (95%) of backgrounds in the respective categories are rejected. The $B^0 \to K^0_S\pi^+\pi^-$ decay selection efficiency is taken from ref. [10]. The efficiencies for the normalisation channel are determined in bins of the Dalitz plane and are reweighted from data using the *sPlot* method [31].

4 Fit model

Two-dimensional extended maximum likelihood fits to the unbinned $K^0_S K^+\pi^-$ and $K^+\pi^-$ mass distributions are used to determine the event yields for the signal channel, while an independent one-dimensional fit to the $K^0_S\pi^+\pi^-$ mass distribution is used for the normalisation channel. The correlation between the two signal mass distributions is checked on simulation. The results do not show significant correlations and therefore the correlation terms are neglected in the fit. Candidates in the long and downstream categories are fitted simultaneously. The signal fit is restricted to candidates in the mass regions $5000 < m(K^0_S K^+\pi^-) < 5800$ MeV/c^2 and $650 < m(K^+\pi^-) < 1200$ MeV/c^2. The fit model consists of signal, non-resonant background, partially reconstructed background and combinatorial background components.

The B^0 and the B^0_s components of the signal are both parametrised as two Gaussian distributions with a power-law tail on each side. For each component the two functions share the peak position and the width parameters. The parameters describing the tails are determined by fits to simulated samples and subsequently fixed in the fit to data. The systematic uncertainty associated with this choice is found to be negligible. The B^0-B^0_s mass difference is fixed to the known value [13]. The K^{*0} mass distribution is parametrised by a relativistic Breit-Wigner function with the peak position and width allowed to vary in the fit.

The components in the B mass model that are non-resonant in $K^+\pi^-$ are parametrised by the same function as the signal, sharing their peak positions and widths with the signal functions. The tail parameters are fixed according to the values obtained from simulation. The non-resonant component of the $K^+\pi^-$ mass distribution is approximated by a normalised linear function as in ref. [11], with the zero point of the function on the abscissa determined by the fit. While the ratio between the non-resonant and the signal components is fixed to be the same for the two K^0_S meson categories, it is independent for the B^0 and the B^0_s candidates.

Backgrounds from partially reconstructed decays are classified into two categories. Decays such as $B \to Dh$ are parametrised by means of ARGUS functions convolved with a Gaussian function in the B candidate mass, and linear functions in the K^{*0} candidate

JHEP01(2016)012

Decay	Downstream		Long	
	Yield	Efficiency (%)	Yield	Efficiency (%)
$B_s^0 \to K_S^0 K^{*0}$	21 ± 6	0.0174 ± 0.0012	25 ± 6	0.0121 ± 0.0008
$B^0 \to K_S^0 K^{*0}$	2 ± 3	0.0183 ± 0.0013	1 ± 2	0.0125 ± 0.0009
$B^0 \to K_S^0 \pi^+\pi^-$	828 ± 41	0.0336 ± 0.0010	341 ± 23	0.0117 ± 0.0009

Table 1. Signal yields obtained from the fits to $K_S^0 K^\pm \pi^\mp$ and $K_S^0 \pi^+\pi^-$ mass distributions and corresponding efficiencies. Only statistical contributions to the uncertainty are reported.

mass. The choice is based on simulation studies and previous findings [10, 11]. In decays such as $B_s^0 \to K^{*0}\overline{K}^{*0}$, where one resonance decays as $K^{*0} \to K^+\pi^-$ while the other decays as $\overline{K}^{*0} \to K_S^0\pi^0$, the B_s^0 mass distribution is described using the same parametrisation as for the previous background, while the invariant mass distribution for K^{*0} candidates is described by a relativistic Breit-Wigner function sharing the peak position and widths with the signal component. The yield for these components are determined in the fit to data.

The combinatorial background is modelled by an exponential function in the B candidate mass distribution and a linear function in the K^{*0} candidate mass distribution. These functions are found to give good agreement with the distributions in the appropriate data sidebands. The slopes of the exponential functions are independent for the long and downstream categories, while the abscissae of the linear functions are the same. All these parameters are allowed to vary in the fit.

The parametrisation used to model the $B^0 \to K_S^0\pi^+\pi^-$ normalisation and the background follow those used to fit the signal mode. In addition two other categories of partially reconstructed backgrounds are included: decays such as $B^0 \to K_S^0\pi^+\pi^-\gamma$ or $B^0 \to \eta' K_S^0$, with $\eta \to \rho^0\gamma$; and misidentified $B_{(s)}^0 \to K_S^0 K^\pm\pi^\mp$ decays. Their parameters are fixed in the fit to the values derived from simulated samples.

The observed $K_S^0 K^{*0}$ and $K_S^0\pi^+\pi^-$ mass distributions and the corresponding fits are shown in figures 1 and 2, respectively. The signal yields are reported in table 1. The B^0 mode is dominated by the non-resonant component. The statistical significance of the B_s^0 signal is determined using Wilks' theorem [32] and by combining the long and the downstream samples. The significance including relevant systematic uncertainties, estimated by repeating the procedure with the signal likelihood convolved with a Gaussian function of width equal to the sum in quadrature of the systematic uncertainties, is 7.1 standard deviations.

5 Systematic uncertainties

The model used to fit data and the limited knowledge in the efficiency determination are possible sources of systematic uncertainty. Many parameters in the fit are fixed to values obtained from fits to simulated data. The associated systematic uncertainties are determined from fits to pseudoexperiments generated assuming alternative values of the relevant parameters, corresponding to variations within uncertainties around their default

JHEP01(2016)012

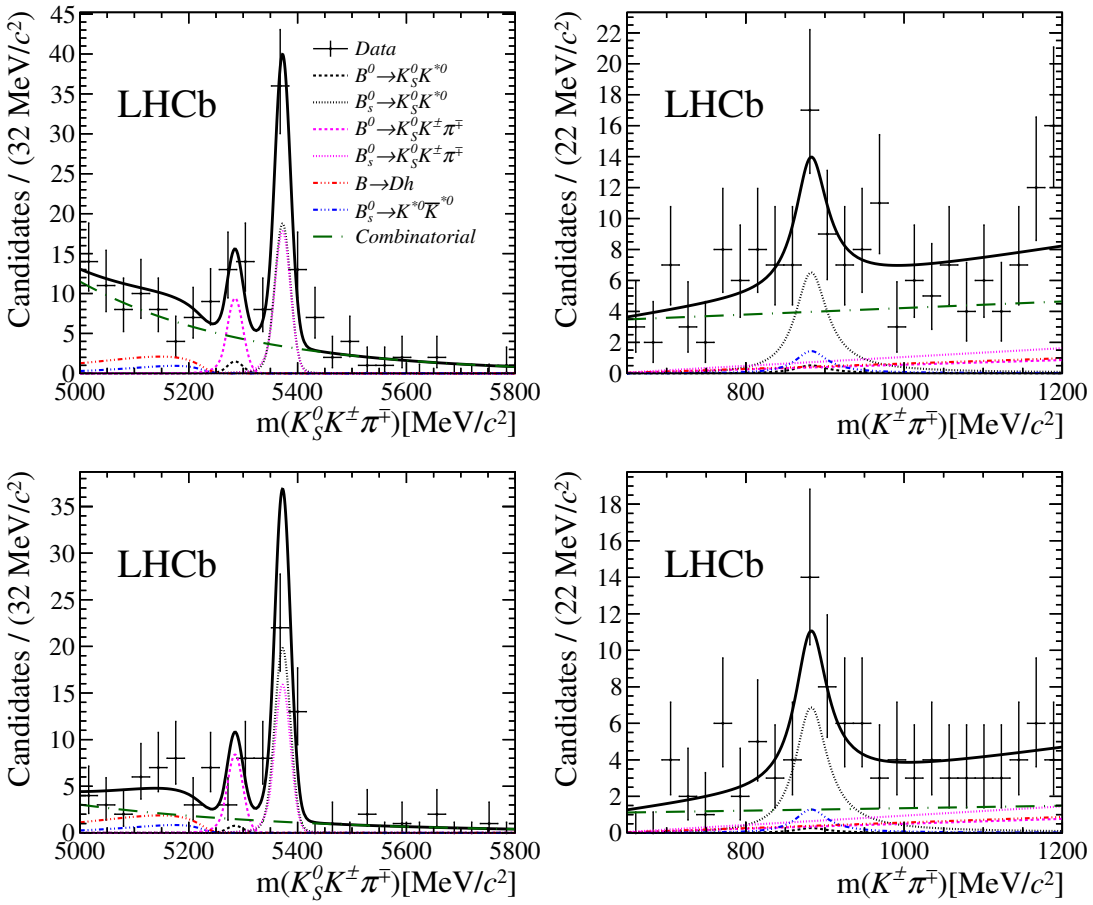

Figure 1. Distribution of (left) $K^0_S K^\pm \pi^\mp$ mass and (right) $K^\pm \pi^\mp$ mass for signal candidates with fit results overlaid for (top) downstream and (bottom) long categories. The data are shown as black points with error bars. The overall fit is represented by the solid black line. The B^0 and B^0_s signal components are the black short-dashed and dotted lines respectively, while the non-resonant components are the magenta short-dashed and dotted lines. The partially reconstructed backgrounds are the red triple-dotted line ($B \to Dh$) and the blue triple-dotted line ($B^0_s \to K^{*0}\overline{K}^{*0}$). The combinatorial background is the green long-dash dotted line.

values. The average difference between the yields determined in the pseudoexperiments and the nominal value is taken as a systematic uncertainty.

The fit model does not account for the possible interference between the P wave of the $K^*(892)^0$ resonance and the S wave from other intermediate states, *e.g.* the non-resonant component or the $K^*(1430)^0$ resonance. The associated systematic uncertainty is determined by exploiting the distribution of $\theta_{K^{*0}}$, defined as the angle between the flight direction of the K^+ in the K^{*0} rest frame with respect to the direction of the boost from the laboratory frame to the K^{*0} rest frame. The $\cos\theta_{K^{*0}}$ distribution is described by a parabola, where the second-order term represents the signal P wave, the constant term is related to the S wave and the first-order term accounts for the interference. Using the *sPlot* technique [31], the $\cos\theta_{K^{*0}}$ distribution of the signal P and S wave is unfolded from the other background components. A fit in the region of positive $\cos\theta_{K^{*0}}$ is performed using

JHEP01(2016)012

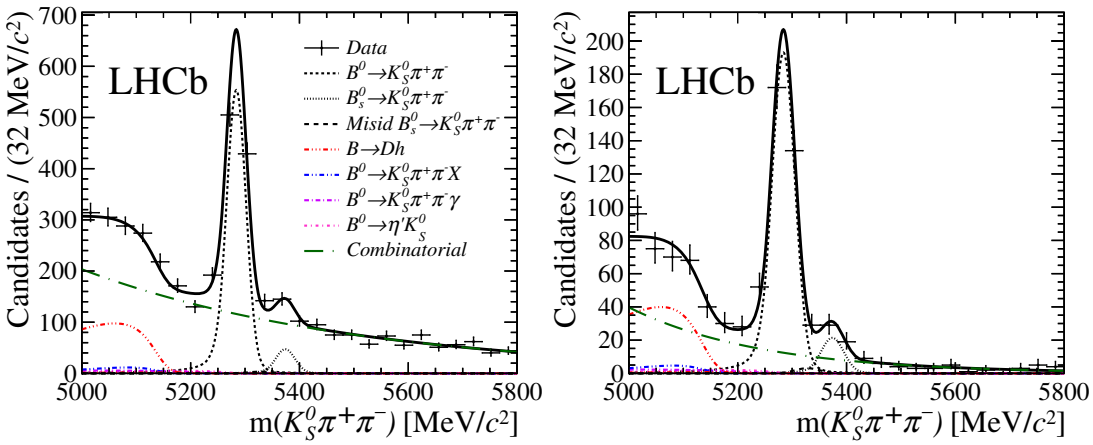

Figure 2. Distribution of $K^0_S\pi^+\pi^-$ mass for signal candidates with fit results overlaid for (left) downstream and (right) long categories. The data are described by the black points with error bars. The overall fit is represented by the solid black line. The B^0 and B^0_s signal components are the black short-dashed and dotted lines. The misidentified B^0_s decay is the black dashed line, respectively. The partially reconstructed backgrounds are the red triple-dotted line ($B \to Dh$), the blue triple-dotted line ($B^0 \to K^0_S\pi^+\pi^-X$), the violet dash single-dotted line ($B^0 \to \eta' K^0_S$) and the pink short-dash single dotted line ($B^0 \to K^0_S\pi^+\pi^-\gamma$). The combinatorial background is the green long-dash dotted line. Some of the contributions are small in the figures.

a second-order polynomial and the systematic uncertainty is determined as the relative difference between the integral of the function when the constant coefficient is allowed to vary and when this coefficient is fixed to zero. Due to the limited size of the $B^0 \to K^0_S K^{*0}$ sample, the relative uncertainty obtained for the $B^0_s \to K^0_S K^{*0}$ decays is also applied to the $B^0 \to K^0_S K^{*0}$ decays.

Potential biases that may be associated with the maximum likelihood estimator are investigated using pseudoexperiments. The systematic uncertainty is determined as the average difference between the nominal value and the fitted yields in the pseudoexperiments.

The impact of the limited size of the simulated samples, used to determine the selection and particle identification efficiencies, is considered as systematic uncertainty. In addition, the hardware trigger is a potential source of systematic uncertainty due to imperfections in the description of data by simulation. A data sample of $D^{*+} \to D^0\pi^\pm$, with $D^0 \to K^-\pi^+$, decays is used to characterise the trigger efficiencies of the pions and kaons, separated according to particle charge, as a function of the transverse energy of the associated cluster in the hadron calorimeter [26, 33]. These data-driven calibration curves are used to weight simulated events in order to determine the efficiency of the hadron trigger.

The effective lifetimes of B^0_s meson reconstructed in a particular decay depend on the *CP*-admixture of the final state because *CP*-even and *CP*-odd eigenstates may have different lifetimes [34]. Since the selection efficiency depends on decay time, this might lead to a source of uncertainty in the measurement. The relative change in efficiency with respect to the nominal value, estimated for the extreme ranges of possible effective lifetime distributions, is assigned as the systematic uncertainty.

JHEP01(2016)012

Source	$\frac{\mathcal{B}(B_s^0 \to K_S^0 K^{*0})}{\mathcal{B}(B^0 \to K_S^0 \pi^+\pi^-)}$		$\frac{\mathcal{B}(B^0 \to K_S^0 K^{*0})}{\mathcal{B}(B^0 \to K_S^0 \pi^+\pi^-)}$	
	Downstream	Long	Downstream	Long
Fit	0.05	0.03	0.20	0.28
Selection efficiency	0.08	0.10	0.08	0.11
PID efficiency	0.01	0.01	0.01	0.01
Trigger	0.07	0.07	0.02	0.09
Lifetime	0.05	0.05	—	—
Total	0.13	0.14	0.22	0.31
f_s/f_d	0.06	0.06	—	—

Table 2. Systematic uncertainties on the relative branching fraction measurement for the two K_S^0 categories. The uncertainties are quoted as fractional contributions of the relative branching fraction and the total is the sum in quadrature of all contributions.

Finally, the uncertainty from the measurement of the fragmentation fractions ratio, f_s/f_d [14–16], is taken into account. A summary of the relative uncertainties on the ratio of branching fractions is given in table 2. The final results reported in section 6 take into account correlations between the two samples; thus the systematic uncertainty for the combined measurement is reduced.

6 Summary and conclusion

A search for $B^0_{(s)} \to K^0_S K^{*0}$ decays is performed by the LHCb experiment using pp data recorded at a centre-of-mass energy of 7TeV, corresponding to an integrated luminosity of $1.0\,\text{fb}^{-1}$. The branching ratios are determined using the $B^0 \to K^0_S \pi^+\pi^-$ decay as a normalisation mode. The measurements are performed separately for the downstream and long K^0_S categories and then combined following refs. [35, 36].

The B^0_s decay is observed for the first time, with a total significance of 7.1 standard deviations. The relative branching fraction is

$$\frac{\mathcal{B}(B^0_s \to K^0_S K^{*0})}{\mathcal{B}(B^0 \to K^0_S \pi^+\pi^-)} = 0.33 \pm 0.07\ (\text{stat}) \pm 0.04\ (\text{syst}) \pm 0.02\ (f_s/f_d).$$

For the B^0 decay, an upper limit at 90% (95%) confidence level (CL) is determined. The likelihood function is convolved with a Gaussian function with standard deviation equal to the total systematic uncertainty, and the upper limit is taken to be the value of the relative branching fraction below which 90% (95%) of the total integral of the likelihood function over non-negative branching ratio values is found. The central value and the upper limit on the relative branching fraction of the decay $B^0 \to K^0_S K^{*0}$ are

$$\begin{aligned}\frac{\mathcal{B}(B^0 \to K^0_S K^{*0})}{\mathcal{B}(B^0 \to K^0_S \pi^+\pi^-)} &= 0.005 \pm 0.007\ (\text{stat}) \pm 0.001\ (\text{syst}),\\ &< 0.020\ (0.021) \text{ at } 90\%\ (95\%)\ \text{CL}.\end{aligned}$$

JHEP01(2016)012

The absolute branching fractions, calculated using the reference value of $\mathcal{B}(B^0 \to K^0\pi^+\pi^-) = (4.96 \pm 0.20) \times 10^{-5}$ [37], determined without using the correlated LHCb measurement. The results are expressed in terms of the sum of final states containing either K^0 or $\bar{K}^0$ mesons

$$\begin{aligned}
\mathcal{B}(B_s^0 \to \bar{K}^0 K^*(892)^0) + \mathcal{B}(B_s^0 \to K^0 \bar{K}^*(892)^0) &= (16.4 \pm 3.4 \pm 1.9 \pm 1.0 \pm 0.7) \times 10^{-6}, \\
\mathcal{B}(B^0 \to \bar{K}^0 K^*(892)^0) + \mathcal{B}(B^0 \to K^0 \bar{K}^*(892)^0) &= (0.25 \pm 0.34 \pm 0.05 \pm 0.01) \times 10^{-6}, \\
&< 0.96\ (1.04) \times 10^{-6} \text{ at } 90\%\ (95\%) \text{ CL},
\end{aligned}$$

where the first uncertainty is statistical, the second systematic, the third due to the ratio of the fragmentation fractions and the fourth due to the uncertainty on the branching fraction of the normalisation decay. These results are in agreement with theoretical predictions [6–8] and can be used to further constrain phenomenological models.

Acknowledgments

We express our gratitude to our colleagues in the CERN accelerator departments for the excellent performance of the LHC. We thank the technical and administrative staff at the LHCb institutes. We acknowledge support from CERN and from the national agencies: CAPES, CNPq, FAPERJ and FINEP (Brazil); NSFC (China); CNRS/IN2P3 (France); BMBF, DFG, HGF and MPG (Germany); INFN (Italy); FOM and NWO (The Netherlands); MNiSW and NCN (Poland); MEN/IFA (Romania); MinES and FANO (Russia); MinECo (Spain); SNSF and SER (Switzerland); NASU (Ukraine); STFC (United Kingdom); NSF (U.S.A.). The Tier1 computing centres are supported by IN2P3 (France), KIT and BMBF (Germany), INFN (Italy), NWO and SURF (The Netherlands), PIC (Spain), GridPP (United Kingdom). We are indebted to the communities behind the multiple open source software packages on which we depend. We are also thankful for the computing resources and the access to software R&D tools provided by Yandex LLC (Russia). Individual groups or members have received support from EPLANET, Marie Skłodowska-Curie Actions and ERC (European Union), Conseil général de Haute-Savoie, Labex ENIGMASS and OCEVU, Région Auvergne (France), RFBR (Russia), XuntaGal and GENCAT (Spain), Royal Society and Royal Commission for the Exhibition of 1851 (United Kingdom). We acknowledge Ulrich Nierste from KIT (Germany) for his assistance on theoretical aspects of the analysis.

References

[1] A. Sakharov, *Violation of CP invariance, C asymmetry, and baryon asymmetry of the Universe*, *J. Exp. Theor. Phys. Lett.* **5** (1967) 24.

[2] N. Cabibbo, *Unitary symmetry and leptonic decays*, *Phys. Rev. Lett.* **10** (1963) 531 [INSPIRE].

JHEP01(2016)012

[3] M. Kobayashi and T. Maskawa, *CP violation in the renormalizable theory of weak interaction*, *Prog. Theor. Phys.* **49** (1973) 652 [INSPIRE].

[4] A. Riotto and M. Trodden, *Recent progress in baryogenesis*, *Ann. Rev. Nucl. Part. Sci.* **49** (1999) 35 [hep-ph/9901362] [INSPIRE].

[5] M. Ciuchini, M. Pierini and L. Silvestrini, *$B(s) \to K^{(*)0}\bar{K}^{(*)0}$ decays: the golden channels for new physics searches*, *Phys. Rev. Lett.* **100** (2008) 031802 [hep-ph/0703137] [INSPIRE].

[6] H.-Y. Cheng and C.-K. Chua, *QCD factorization for charmless hadronic B_s decays revisited*, *Phys. Rev.* **D 80** (2009) 114026 [arXiv:0910.5237] [INSPIRE].

[7] A. Ali et al., *Charmless non-leptonic B_s decays to PP, PV and VV final states in the pQCD approach*, *Phys. Rev.* **D 76** (2007) 074018 [hep-ph/0703162] [INSPIRE].

[8] F. Su, Y.-L. Wu, C. Zhuang and Y.-B. Yang, *Charmless $B_s \to PP, PV, VV$ decays based on the six-quark effective hamiltonian with strong phase effects II*, *Eur. Phys. J.* **C 72** (2012) 1914 [arXiv:1107.0136] [INSPIRE].

[9] R. Dalitz, *On the analysis of τ-meson data and the nature of the τ-meson*, *Phil.Mag.* **44** (1953) 1068.

[10] LHCb collaboration, *Study of $B^0_{(s)} \to K^0_S h^+ h'^-$ decays with first observation of $B^0_s \to K^0_S K^\pm \pi^\mp$ and $B^0_s \to K^0_S \pi^+ \pi^-$*, *JHEP* **10** (2013) 143 [arXiv:1307.7648] [INSPIRE].

[11] LHCb collaboration, *Observation of $B^0_s \to K^{*\pm} K^\mp$ and evidence for $B^0_s \to K^{*-}\pi^+$ decays*, *New J. Phys.* **16** (2014) 123001 [arXiv:1407.7704] [INSPIRE].

[12] BaBar collaboration, B. Aubert et al., *Search for the decay of a B^0 or anti-B^0 meson to $\bar{K}^{*0}K^0$ or K^{*0} $\bar{K}^0$*, *Phys. Rev.* **D 74** (2006) 072008 [hep-ex/0606050] [INSPIRE].

[13] Particle Data Group collaboration, K.A. Olive et al., *Review of particle physics*, *Chin. Phys.* **C 38** (2014) 090001 [INSPIRE].

[14] LHCb collaboration, *Measurement of b-hadron production fractions in 7 TeV pp collisions*, *Phys. Rev.* **D 85** (2012) 032008 [arXiv:1111.2357] [INSPIRE].

[15] LHCb collaboration, *Measurement of the fragmentation fraction ratio f_s/f_d and its dependence on B meson kinematics*, *JHEP* **04** (2013) 001 [arXiv:1301.5286] [INSPIRE].

[16] LHCb collaboration, *Updated average f_s/f_d b-hadron production fraction ratio for 7 TeV pp collisions*, LHCb-CONF-2013-011 (2013).

[17] LHCb collaboration, *The LHCb detector at the LHC*, 2008 *JINST* **3** S08005 [INSPIRE].

[18] LHCb collaboration, *LHCb detector performance*, *Int. J. Mod. Phys.* **A 30** (2015) 1530022 [arXiv:1412.6352] [INSPIRE].

[19] T. Sjöstrand, S. Mrenna and P.Z. Skands, *PYTHIA 6.4 physics and manual*, *JHEP* **05** (2006) 026 [hep-ph/0603175] [INSPIRE].

[20] LHCb collaboration, *Handling of the generation of primary events in Gauss, the LHCb simulation framework*, *J. Phys. Conf. Ser.* **331** (2011) 032047 [INSPIRE].

[21] D.J. Lange, *The EvtGen particle decay simulation package*, *Nucl. Instrum. Meth.* **A 462** (2001) 152 [INSPIRE].

[22] P. Golonka and Z. Was, *PHOTOS Monte Carlo: a precision tool for QED corrections in Z and W decays*, *Eur. Phys. J.* **C 45** (2006) 97 [hep-ph/0506026] [INSPIRE].

JHEP01(2016)012

[23] GEANT4 collaboration, J. Allison et al., *GEANT4 developments and applications*, *IEEE Trans. Nucl. Sci.* **53** (2006) 270.

[24] GEANT4 collaboration, S. Agostinelli et al., *GEANT4: a simulation toolkit*, *Nucl. Instrum. Meth.* **A 506** (2003) 250 [INSPIRE].

[25] LHCb collaboration, *The LHCb simulation application, Gauss: design, evolution and experience*, *J. Phys. Conf. Ser.* **331** (2011) 032023 [INSPIRE].

[26] R. Aaij et al., *The LHCb trigger and its performance in 2011*, 2013 *JINST* **8** P04022 [arXiv:1211.3055] [INSPIRE].

[27] V.V. Gligorov and M. Williams, *Efficient, reliable and fast high-level triggering using a bonsai boosted decision tree*, 2013 *JINST* **8** P02013 [arXiv:1210.6861] [INSPIRE].

[28] L. Breiman, J.H. Friedman, R.A. Olshen and C.J. Stone, *Classification and regression trees*, Wadsworth international group, Belmont U.S.A. (1984).

[29] R.E. Schapire and Y. Freund, *A decision-theoretic generalization of on-line learning and an application to boosting*, *Jour. Comp. Syst. Sci.* **55** (1997) 119.

[30] G. Punzi, *Sensitivity of searches for new signals and its optimization*, *eConf* **C 030908** (2003) MODT002 [physics/0308063] [INSPIRE].

[31] M. Pivk and F.R. Le Diberder, *SPlot: a statistical tool to unfold data distributions*, *Nucl. Instrum. Meth.* **A 555** (2005) 356 [physics/0402083] [INSPIRE].

[32] S. S. Wilks, *The large-sample distribution of the likelihood ratio for testing composite hypotheses*, *Ann. Math.Statist.* **9** (1938) 60.

[33] A. Martin Sanchez, *CP violation studies on the $B^0 \to DK^{*0}$ decays and hadronic trigger performance with the LHCb detector at CERN*, Ph.D. thesis, Université Paris-sud XI, Paris, France (2013).

[34] I. Dunietz, R. Fleischer and U. Nierste, *In pursuit of new physics with B_s decays*, *Phys. Rev.* **D 63** (2001) 114015 [hep-ph/0012219].

[35] L. Lyons, D. Gibaut and P. Clifford, *How to combine correlated estimates of a single physical quantity*, *Nucl. Instrum. Meth.* **A 270** (1988) 110 [INSPIRE].

[36] A. Valassi, *Combining correlated measurements of several different physical quantities*, *Nucl. Instrum. Meth.* **A 500** (2003) 391 [INSPIRE].

[37] PARTICLE DATA GROUP collaboration, J. Beringer et al., *Review of particle physics*, *Phys. Rev.* **D 86** (2012) 010001 [INSPIRE].

JHEP01(2016)012

The LHCb collaboration

R. Aaij[38], B. Adeva[37], M. Adinolfi[46], A. Affolder[52], Z. Ajaltouni[5], S. Akar[6], J. Albrecht[9], F. Alessio[38], M. Alexander[51], S. Ali[41], G. Alkhazov[30], P. Alvarez Cartelle[53], A.A. Alves Jr[57], S. Amato[2], S. Amerio[22], Y. Amhis[7], L. An[3], L. Anderlini[17,g], J. Anderson[40], M. Andreotti[16,f], J.E. Andrews[58], R.B. Appleby[54], O. Aquines Gutierrez[10], F. Archilli[38], P. d'Argent[11], A. Artamonov[35], M. Artuso[59], E. Aslanides[6], G. Auriemma[25,n], M. Baalouch[5], S. Bachmann[11], J.J. Back[48], A. Badalov[36], C. Baesso[60], W. Baldini[16,38], R.J. Barlow[54], C. Barschel[38], S. Barsuk[7], W. Barter[38], V. Batozskaya[28], V. Battista[39], A. Bay[39], L. Beaucourt[4], J. Beddow[51], F. Bedeschi[23], I. Bediaga[1], L.J. Bel[41], I. Belyaev[31], E. Ben-Haim[8], G. Bencivenni[18], S. Benson[38], J. Benton[46], A. Berezhnoy[32], R. Bernet[40], A. Bertolin[22], M.-O. Bettler[38], M. van Beuzekom[41], A. Bien[11], S. Bifani[45], T. Bird[54], A. Birnkraut[9], A. Bizzeti[17,i], T. Blake[48], F. Blanc[39], J. Blouw[10], S. Blusk[59], V. Bocci[25], A. Bondar[34], N. Bondar[30,38], W. Bonivento[15], S. Borghi[54], M. Borsato[7], T.J.V. Bowcock[52], E. Bowen[40], C. Bozzi[16], S. Braun[11], D. Brett[54], M. Britsch[10], T. Britton[59], J. Brodzicka[54], N.H. Brook[46], A. Bursche[40], J. Buytaert[38], S. Cadeddu[15], R. Calabrese[16,f], M. Calvi[20,k], M. Calvo Gomez[36,p], P. Campana[18], D. Campora Perez[38], L. Capriotti[54], A. Carbone[14,d], G. Carboni[24,l], R. Cardinale[19,j], A. Cardini[15], P. Carniti[20], L. Carson[50], K. Carvalho Akiba[2,38], R. Casanova Mohr[36], G. Casse[52], L. Cassina[20,k], L. Castillo Garcia[38], M. Cattaneo[38], Ch. Cauet[9], G. Cavallero[19], R. Cenci[23,t], M. Charles[8], Ph. Charpentier[38], M. Chefdeville[4], S. Chen[54], S.-F. Cheung[55], N. Chiapolini[40], M. Chrzaszcz[40], X. Cid Vidal[38], G. Ciezarek[41], P.E.L. Clarke[50], M. Clemencic[38], H.V. Cliff[47], J. Closier[38], V. Coco[38], J. Cogan[6], E. Cogneras[5], V. Cogoni[15,e], L. Cojocariu[29], G. Collazuol[22], P. Collins[38], A. Comerma-Montells[11], A. Contu[15,38], A. Cook[46], M. Coombes[46], S. Coquereau[8], G. Corti[38], M. Corvo[16,f], B. Couturier[38], G.A. Cowan[50], D.C. Craik[48], A. Crocombe[48], M. Cruz Torres[60], S. Cunliffe[53], R. Currie[53], C. D'Ambrosio[38], J. Dalseno[46], P.N.Y. David[41], A. Davis[57], K. De Bruyn[41], S. De Capua[54], M. De Cian[11], J.M. De Miranda[1], L. De Paula[2], W. De Silva[57], P. De Simone[18], C.-T. Dean[51], D. Decamp[4], M. Deckenhoff[9], L. Del Buono[8], N. Déléage[4], D. Derkach[55], O. Deschamps[5], F. Dettori[38], B. Dey[40], A. Di Canto[38], F. Di Ruscio[24], H. Dijkstra[38], S. Donleavy[52], F. Dordei[11], M. Dorigo[39], A. Dosil Suárez[37], D. Dossett[48], A. Dovbnya[43], K. Dreimanis[52], L. Dufour[41], G. Dujany[54], F. Dupertuis[39], P. Durante[38], R. Dzhelyadin[35], A. Dziurda[26], A. Dzyuba[30], S. Easo[49,38], U. Egede[53], V. Egorychev[31], S. Eidelman[34], S. Eisenhardt[50], U. Eitschberger[9], R. Ekelhof[9], L. Eklund[51], I. El Rifai[5], Ch. Elsasser[40], S. Ely[59], S. Esen[11], H.M. Evans[47], T. Evans[55], A. Falabella[14], C. Färber[11], C. Farinelli[41], N. Farley[45], S. Farry[52], R. Fay[52], D. Ferguson[50], V. Fernandez Albor[37], F. Ferrari[14], F. Ferreira Rodrigues[1], M. Ferro-Luzzi[38], S. Filippov[33], M. Fiore[16,38,f], M. Fiorini[16,f], M. Firlej[27], C. Fitzpatrick[39], T. Fiutowski[27], K. Fohl[38], P. Fol[53], M. Fontana[10], F. Fontanelli[19,j], R. Forty[38], O. Francisco[2], M. Frank[38], C. Frei[38], M. Frosini[17], J. Fu[21], E. Furfaro[24,l], A. Gallas Torreira[37], D. Galli[14,d], S. Gallorini[22,38], S. Gambetta[50], M. Gandelman[2], P. Gandini[55], Y. Gao[3], J. García Pardiñas[37], J. Garofoli[59], J. Garra Tico[47], L. Garrido[36], D. Gascon[36], C. Gaspar[38], R. Gauld[55], L. Gavardi[9], G. Gazzoni[5], A. Geraci[21,v], D. Gerick[11], E. Gersabeck[11], M. Gersabeck[54], T. Gershon[48], Ph. Ghez[4], A. Gianelle[22], S. Giani[39], V. Gibson[47], O. G. Girard[39], L. Giubega[29], V.V. Gligorov[38], C. Göbel[60], D. Golubkov[31], A. Golutvin[53,31,38], A. Gomes[1,a], C. Gotti[20,k], M. Grabalosa Gándara[5], R. Graciani Diaz[36], L.A. Granado Cardoso[38], E. Graugés[36], E. Graverini[40], G. Graziani[17], A. Grecu[29], E. Greening[55], S. Gregson[47], P. Griffith[45], L. Grillo[11], O. Grünberg[63], B. Gui[59], E. Gushchin[33], Yu. Guz[35,38], T. Gys[38], C. Hadjivasiliou[59], G. Haefeli[39], C. Haen[38], S.C. Haines[47], S. Hall[53], B. Hamilton[58], T. Hampson[46], X. Han[11], S. Hansmann-Menzemer[11], N. Harnew[55], S.T. Harnew[46], J. Harrison[54], J. He[38], T. Head[39], V. Heijne[41], K. Hennessy[52], P. Henrard[5], L. Henry[8], J.A. Hernando Morata[37],

JHEP01(2016)012

E. van Herwijnen[38], M. Heß[63], A. Hicheur[2], D. Hill[55], M. Hoballah[5], C. Hombach[54], W. Hulsbergen[41], T. Humair[53], N. Hussain[55], D. Hutchcroft[52], D. Hynds[51], M. Idzik[27], P. Ilten[56], R. Jacobsson[38], A. Jaeger[11], J. Jalocha[55], E. Jans[41], A. Jawahery[58], F. Jing[3], M. John[55], D. Johnson[38], C.R. Jones[47], C. Joram[38], B. Jost[38], N. Jurik[59], S. Kandybei[43], W. Kanso[6], M. Karacson[38], T.M. Karbach[38,†], S. Karodia[51], M. Kelsey[59], I.R. Kenyon[45], M. Kenzie[38], T. Ketel[42], B. Khanji[20,38,k], C. Khurewathanakul[39], S. Klaver[54], K. Klimaszewski[28], O. Kochebina[7], M. Kolpin[11], I. Komarov[39], R.F. Koopman[42], P. Koppenburg[41,38], L. Kravchuk[33], K. Kreplin[11], M. Kreps[48], G. Krocker[11], P. Krokovny[34], F. Kruse[9], W. Kucewicz[26,o], M. Kucharczyk[26], V. Kudryavtsev[34], A. K. Kuonen[39], K. Kurek[28], T. Kvaratskheliya[31], V.N. La Thi[39], D. Lacarrere[38], G. Lafferty[54], A. Lai[15], D. Lambert[50], R.W. Lambert[42], G. Lanfranchi[18], C. Langenbruch[48], B. Langhans[38], T. Latham[48], C. Lazzeroni[45], R. Le Gac[6], J. van Leerdam[41], J.-P. Lees[4], R. Lefèvre[5], A. Leflat[32,38], J. Lefrançois[7], O. Leroy[6], T. Lesiak[26], B. Leverington[11], Y. Li[7], T. Likhomanenko[65,64], M. Liles[52], R. Lindner[38], C. Linn[38], F. Lionetto[40], B. Liu[15], X. Liu[3], S. Lohn[38], I. Longstaff[51], J.H. Lopes[2], D. Lucchesi[22,r], M. Lucio Martinez[37], H. Luo[50], A. Lupato[22], E. Luppi[16,f], O. Lupton[55], F. Machefert[7], F. Maciuc[29], O. Maev[30], K. Maguire[54], S. Malde[55], A. Malinin[64], G. Manca[7], G. Mancinelli[6], P. Manning[59], A. Mapelli[38], J. Maratas[5], J.F. Marchand[4], U. Marconi[14], C. Marin Benito[36], P. Marino[23,38,t], R. Märki[39], J. Marks[11], G. Martellotti[25], M. Martinelli[39], D. Martinez Santos[42], F. Martinez Vidal[66], D. Martins Tostes[2], A. Massafferri[1], R. Matev[38], A. Mathad[48], Z. Mathe[38], C. Matteuzzi[20], K. Matthieu[11], A. Mauri[40], B. Maurin[39], A. Mazurov[45], M. McCann[53], J. McCarthy[45], A. McNab[54], R. McNulty[12], B. Meadows[57], F. Meier[9], M. Meissner[11], M. Merk[41], D.A. Milanes[62], M.-N. Minard[4], D.S. Mitzel[11], J. Molina Rodriguez[60], S. Monteil[5], M. Morandin[22], P. Morawski[27], A. Mordà[6], M.J. Morello[23,t], J. Moron[27], A.B. Morris[50], R. Mountain[59], F. Muheim[50], J. Müller[9], K. Müller[40], V. Müller[9], M. Mussini[14], B. Muster[39], P. Naik[46], T. Nakada[39], R. Nandakumar[49], I. Nasteva[2], M. Needham[50], N. Neri[21], S. Neubert[11], N. Neufeld[38], M. Neuner[11], A.D. Nguyen[39], T.D. Nguyen[39], C. Nguyen-Mau[39,q], V. Niess[5], R. Niet[9], N. Nikitin[32], T. Nikodem[11], D. Ninci[23], A. Novoselov[35], D.P. O'Hanlon[48], A. Oblakowska-Mucha[27], V. Obraztsov[35], S. Ogilvy[51], O. Okhrimenko[44], R. Oldeman[15,e], C.J.G. Onderwater[67], B. Osorio Rodrigues[1], J.M. Otalora Goicochea[2], A. Otto[38], P. Owen[53], A. Oyanguren[66], A. Palano[13,c], F. Palombo[21,u], M. Palutan[18], J. Panman[38], A. Papanestis[49], M. Pappagallo[51], L.L. Pappalardo[16,f], C. Parkes[54], G. Passaleva[17], G.D. Patel[52], M. Patel[53], C. Patrignani[19,j], A. Pearce[54,49], A. Pellegrino[41], G. Penso[25,m], M. Pepe Altarelli[38], S. Perazzini[14,d], P. Perret[5], L. Pescatore[45], K. Petridis[46], A. Petrolini[19,j], E. Picatoste Olloqui[36], B. Pietrzyk[4], T. Pilař[48], D. Pinci[25], A. Pistone[19], A. Piucci[11], S. Playfer[50], M. Plo Casasus[37], T. Poikela[38], F. Polci[8], A. Poluektov[48,34], I. Polyakov[31], E. Polycarpo[2], A. Popov[35], D. Popov[10,38], B. Popovici[29], C. Potterat[2], E. Price[46], J.D. Price[52], J. Prisciandaro[39], A. Pritchard[52], C. Prouve[46], V. Pugatch[44], A. Puig Navarro[39], G. Punzi[23,s], W. Qian[4], R. Quagliani[7,46], B. Rachwal[26], J.H. Rademacker[46], B. Rakotomiaramanana[39], M. Rama[23], M.S. Rangel[2], I. Raniuk[43], N. Rauschmayr[38], G. Raven[42], F. Redi[53], S. Reichert[54], M.M. Reid[48], A.C. dos Reis[1], S. Ricciardi[49], S. Richards[46], M. Rihl[38], K. Rinnert[52], V. Rives Molina[36], P. Robbe[7,38], A.B. Rodrigues[1], E. Rodrigues[54], J.A. Rodriguez Lopez[62], P. Rodriguez Perez[54], S. Roiser[38], V. Romanovsky[35], A. Romero Vidal[37], M. Rotondo[22], J. Rouvinet[39], T. Ruf[38], H. Ruiz[36], P. Ruiz Valls[66], J.J. Saborido Silva[37], N. Sagidova[30], P. Sail[51], B. Saitta[15,e], V. Salustino Guimaraes[2], C. Sanchez Mayordomo[66], B. Sanmartin Sedes[37], R. Santacesaria[25], C. Santamarina Rios[37], M. Santimaria[18], E. Santovetti[24,l], A. Sarti[18,m], C. Satriano[25,n], A. Satta[24], D.M. Saunders[46], D. Savrina[31,32], M. Schiller[38], H. Schindler[38], M. Schlupp[9], M. Schmelling[10], T. Schmelzer[9], B. Schmidt[38], O. Schneider[39], A. Schopper[38], M. Schubiger[39], M.-H. Schune[7], R. Schwemmer[38], B. Sciascia[18], A. Sciubba[25,m], A. Semennikov[31], I. Sepp[53],

JHEP01(2016)012

N. Serra[40], J. Serrano[6], L. Sestini[22], P. Seyfert[11], M. Shapkin[35], I. Shapoval[16,43,f], Y. Shcheglov[30], T. Shears[52], L. Shekhtman[34], V. Shevchenko[64], A. Shires[9], R. Silva Coutinho[48], G. Simi[22], M. Sirendi[47], N. Skidmore[46], I. Skillicorn[51], T. Skwarnicki[59], E. Smith[55,49], E. Smith[53], I. T. Smith[50], J. Smith[47], M. Smith[54], H. Snoek[41], M.D. Sokoloff[57,38], F.J.P. Soler[51], F. Soomro[39], D. Souza[46], B. Souza De Paula[2], B. Spaan[9], P. Spradlin[51], S. Sridharan[38], F. Stagni[38], M. Stahl[11], S. Stahl[38], O. Steinkamp[40], O. Stenyakin[35], F. Sterpka[59], S. Stevenson[55], S. Stoica[29], S. Stone[59], B. Storaci[40], S. Stracka[23,t], M. Straticiuc[29], U. Straumann[40], L. Sun[57], W. Sutcliffe[53], K. Swientek[27], S. Swientek[9], V. Syropoulos[42], M. Szczekowski[28], P. Szczypka[39,38], T. Szumlak[27], S. T'Jampens[4], T. Tekampe[9], M. Teklishyn[7], G. Tellarini[16,f], F. Teubert[38], C. Thomas[55], E. Thomas[38], J. van Tilburg[41], V. Tisserand[4], M. Tobin[39], J. Todd[57], S. Tolk[42], L. Tomassetti[16,f], D. Tonelli[38], S. Topp-Joergensen[55], N. Torr[55], E. Tournefier[4], S. Tourneur[39], K. Trabelsi[39], M.T. Tran[39], M. Tresch[40], A. Trisovic[38], A. Tsaregorodtsev[6], P. Tsopelas[41], N. Tuning[41,38], A. Ukleja[28], A. Ustyuzhanin[65,64], U. Uwer[11], C. Vacca[15,e], V. Vagnoni[14], G. Valenti[14], A. Vallier[7], R. Vazquez Gomez[18], P. Vazquez Regueiro[37], C. Vázquez Sierra[37], S. Vecchi[16], J.J. Velthuis[46], M. Veltri[17,h], G. Veneziano[39], M. Vesterinen[11], B. Viaud[7], D. Vieira[2], M. Vieites Diaz[37], X. Vilasis-Cardona[36,p], A. Vollhardt[40], D. Volyanskyy[10], D. Voong[46], A. Vorobyev[30], V. Vorobyev[34], C. Voß[63], J.A. de Vries[41], R. Waldi[63], C. Wallace[48], R. Wallace[12], J. Walsh[23], S. Wandernoth[11], J. Wang[59], D.R. Ward[47], N.K. Watson[45], D. Websdale[53], A. Weiden[40], M. Whitehead[48], D. Wiedner[11], G. Wilkinson[55,38], M. Wilkinson[59], M. Williams[38], M.P. Williams[45], M. Williams[56], T. Williams[45], F.F. Wilson[49], J. Wimberley[58], J. Wishahi[9], W. Wislicki[28], M. Witek[26], G. Wormser[7], S.A. Wotton[47], S. Wright[47], K. Wyllie[38], Y. Xie[61], Z. Xu[39], Z. Yang[3], J. Yu[61], X. Yuan[34], O. Yushchenko[35], M. Zangoli[14], M. Zavertyaev[10,b], L. Zhang[3], Y. Zhang[3], A. Zhelezov[11], A. Zhokhov[31], L. Zhong[3]

[1] *Centro Brasileiro de Pesquisas Físicas (CBPF), Rio de Janeiro, Brazil*
[2] *Universidade Federal do Rio de Janeiro (UFRJ), Rio de Janeiro, Brazil*
[3] *Center for High Energy Physics, Tsinghua University, Beijing, China*
[4] *LAPP, Université Savoie Mont-Blanc, CNRS/IN2P3, Annecy-Le-Vieux, France*
[5] *Clermont Université, Université Blaise Pascal, CNRS/IN2P3, LPC, Clermont-Ferrand, France*
[6] *CPPM, Aix-Marseille Université, CNRS/IN2P3, Marseille, France*
[7] *LAL, Université Paris-Sud, CNRS/IN2P3, Orsay, France*
[8] *LPNHE, Université Pierre et Marie Curie, Université Paris Diderot, CNRS/IN2P3, Paris, France*
[9] *Fakultät Physik, Technische Universität Dortmund, Dortmund, Germany*
[10] *Max-Planck-Institut für Kernphysik (MPIK), Heidelberg, Germany*
[11] *Physikalisches Institut, Ruprecht-Karls-Universität Heidelberg, Heidelberg, Germany*
[12] *School of Physics, University College Dublin, Dublin, Ireland*
[13] *Sezione INFN di Bari, Bari, Italy*
[14] *Sezione INFN di Bologna, Bologna, Italy*
[15] *Sezione INFN di Cagliari, Cagliari, Italy*
[16] *Sezione INFN di Ferrara, Ferrara, Italy*
[17] *Sezione INFN di Firenze, Firenze, Italy*
[18] *Laboratori Nazionali dell'INFN di Frascati, Frascati, Italy*
[19] *Sezione INFN di Genova, Genova, Italy*
[20] *Sezione INFN di Milano Bicocca, Milano, Italy*
[21] *Sezione INFN di Milano, Milano, Italy*
[22] *Sezione INFN di Padova, Padova, Italy*
[23] *Sezione INFN di Pisa, Pisa, Italy*
[24] *Sezione INFN di Roma Tor Vergata, Roma, Italy*
[25] *Sezione INFN di Roma La Sapienza, Roma, Italy*
[26] *Henryk Niewodniczanski Institute of Nuclear Physics Polish Academy of Sciences, Kraków, Poland*

JHEP01(2016)012

[27] AGH - University of Science and Technology, Faculty of Physics and Applied Computer Science, Kraków, Poland
[28] National Center for Nuclear Research (NCBJ), Warsaw, Poland
[29] Horia Hulubei National Institute of Physics and Nuclear Engineering, Bucharest-Magurele, Romania
[30] Petersburg Nuclear Physics Institute (PNPI), Gatchina, Russia
[31] Institute of Theoretical and Experimental Physics (ITEP), Moscow, Russia
[32] Institute of Nuclear Physics, Moscow State University (SINP MSU), Moscow, Russia
[33] Institute for Nuclear Research of the Russian Academy of Sciences (INR RAN), Moscow, Russia
[34] Budker Institute of Nuclear Physics (SB RAS) and Novosibirsk State University, Novosibirsk, Russia
[35] Institute for High Energy Physics (IHEP), Protvino, Russia
[36] Universitat de Barcelona, Barcelona, Spain
[37] Universidad de Santiago de Compostela, Santiago de Compostela, Spain
[38] European Organization for Nuclear Research (CERN), Geneva, Switzerland
[39] Ecole Polytechnique Fédérale de Lausanne (EPFL), Lausanne, Switzerland
[40] Physik-Institut, Universität Zürich, Zürich, Switzerland
[41] Nikhef National Institute for Subatomic Physics, Amsterdam, The Netherlands
[42] Nikhef National Institute for Subatomic Physics and VU University Amsterdam, Amsterdam, The Netherlands
[43] NSC Kharkiv Institute of Physics and Technology (NSC KIPT), Kharkiv, Ukraine
[44] Institute for Nuclear Research of the National Academy of Sciences (KINR), Kyiv, Ukraine
[45] University of Birmingham, Birmingham, United Kingdom
[46] H.H. Wills Physics Laboratory, University of Bristol, Bristol, United Kingdom
[47] Cavendish Laboratory, University of Cambridge, Cambridge, United Kingdom
[48] Department of Physics, University of Warwick, Coventry, United Kingdom
[49] STFC Rutherford Appleton Laboratory, Didcot, United Kingdom
[50] School of Physics and Astronomy, University of Edinburgh, Edinburgh, United Kingdom
[51] School of Physics and Astronomy, University of Glasgow, Glasgow, United Kingdom
[52] Oliver Lodge Laboratory, University of Liverpool, Liverpool, United Kingdom
[53] Imperial College London, London, United Kingdom
[54] School of Physics and Astronomy, University of Manchester, Manchester, United Kingdom
[55] Department of Physics, University of Oxford, Oxford, United Kingdom
[56] Massachusetts Institute of Technology, Cambridge, MA, United States
[57] University of Cincinnati, Cincinnati, OH, United States
[58] University of Maryland, College Park, MD, United States
[59] Syracuse University, Syracuse, NY, United States
[60] Pontifícia Universidade Católica do Rio de Janeiro (PUC-Rio), Rio de Janeiro, Brazil, associated to[2]
[61] Institute of Particle Physics, Central China Normal University, Wuhan, Hubei, China, associated to[3]
[62] Departamento de Fisica , Universidad Nacional de Colombia, Bogota, Colombia, associated to[8]
[63] Institut für Physik, Universität Rostock, Rostock, Germany, associated to[11]
[64] National Research Centre Kurchatov Institute, Moscow, Russia, associated to[31]
[65] Yandex School of Data Analysis, Moscow, Russia, associated to[31]
[66] Instituto de Fisica Corpuscular (IFIC), Universitat de Valencia-CSIC, Valencia, Spain, associated to[36]
[67] Van Swinderen Institute, University of Groningen, Groningen, The Netherlands, associated to[41]

[a] Universidade Federal do Triângulo Mineiro (UFTM), Uberaba-MG, Brazil
[b] P.N. Lebedev Physical Institute, Russian Academy of Science (LPI RAS), Moscow, Russia
[c] Università di Bari, Bari, Italy

JHEP01(2016)012

[d] *Università di Bologna, Bologna, Italy*
[e] *Università di Cagliari, Cagliari, Italy*
[f] *Università di Ferrara, Ferrara, Italy*
[g] *Università di Firenze, Firenze, Italy*
[h] *Università di Urbino, Urbino, Italy*
[i] *Università di Modena e Reggio Emilia, Modena, Italy*
[j] *Università di Genova, Genova, Italy*
[k] *Università di Milano Bicocca, Milano, Italy*
[l] *Università di Roma Tor Vergata, Roma, Italy*
[m] *Università di Roma La Sapienza, Roma, Italy*
[n] *Università della Basilicata, Potenza, Italy*
[o] *AGH - University of Science and Technology, Faculty of Computer Science, Electronics and Telecommunications, Kraków, Poland*
[p] *LIFAELS, La Salle, Universitat Ramon Llull, Barcelona, Spain*
[q] *Hanoi University of Science, Hanoi, Viet Nam*
[r] *Università di Padova, Padova, Italy*
[s] *Università di Pisa, Pisa, Italy*
[t] *Scuola Normale Superiore, Pisa, Italy*
[u] *Università degli Studi di Milano, Milano, Italy*
[v] *Politecnico di Milano, Milano, Italy* [†]*Deceased*

JHEP01(2016)012